Crystal Structure of $La_2Mo_2O_9$, a New Fast Oxide−Ion Conductor

F. Goutenoire,* O. Isnard,† R. Retoux, and P. Lacorre

Laboratoire des Fluorures, UPRES-A CNRS 6010, Université du Maine, 72085 Le Mans Cedex 9, France

Received January 4, 2000. Revised Manuscript Received June 2, 2000

The crystal structure of the new fast oxide-ion conductor $La_2Mo_2O_9$ (ionic conductivity of 0.06 S cm^{-1} at 800 °C) has been studied. This compound presents a reversible phase transformation around 580 °C from a low-temperature form α-$La_2Mo_2O_9$ to a high-temperature form β-$La_2Mo_2O_9$. The high-temperature form β-$La_2Mo_2O_9$ has a cubic structure (at 617 °C, space group $P2_13$; $a = 7.2014(5)$ Å; $Z = 2$; $R_{Bragg} = 5.8\%$, $R_p = 10.9\%$, $R_{wp} = 6.5\%$, $\chi^2 = 7.7$) which derives from that of β-$SnWO_4$. Partial site occupation by oxygen atoms, strongly anisotropic thermal factors, and short-range order with a distance characteristic of O−O pairs have been evidenced. An original concept is proposed for the origin of oxide−ion conduction in this compound, which could be applied to the design of new oxide−ion conductors. The low-temperature form α-$La_2Mo_2O_9$ exhibits a slight monoclinic distortion and a large superstructure relative to β-$La_2Mo_2O_9$ ($2 \times 3 \times 4$), most probably due to the localization of oxygen atoms. The large cell (∼8800 $Å^3$) did not allow us to determine the crystal structure of α-$La_2Mo_2O_9$.

Introduction

Fast oxide−ion conductors keep on attracting considerable interest because of their important fields of application, including oxygen sensors and oxygen pumping devices (for recent reviews, see for instance refs 1−3 and references therein). In a previous paper,[4] we have reported the existence of a new series of oxide ion conductors (the LAMOX family), issued from various cationic substitutions on the parent compound, lanthanum molybdate $La_2Mo_2O_9$, which exhibits an ionic conductivity as high as 6×10^{-2} S cm^{-1} at 800 °C. Such a compound, first reported by Fournier et al.[5] who prepared it using conventional ceramic synthesis, has been known since 1970. These authors reported that the diffraction pattern of this compound can be indexed in a cubic system with parameter $a = 7.155 \pm 0.005$ Å. More recently, some of us have shown that it is possible to prepare $La_2Mo_2O_9$ by direct ball milling synthesis[6] and that its reduction under hydrogen leads to the formation of a new, perovskite-related, compound $La_7Mo_7O_{30}$.[7] Lately, W. Kuang et al.[8] reported the preparation of nanoscaled powder of $La_2Mo_2O_9$ and studied its enhanced catalytic activity. However, up to now, its structure was still unknown. In our previous study,[4] we established that $La_2Mo_2O_9$ undergoes a phase transition from a low-temperature slightly distorted form (α-$La_2Mo_2O_9$) to a high-temperature, more conducting cubic form (β-$La_2Mo_2O_9$).

The aim of this work was to determine the crystal structures of $La_2Mo_2O_9$ using X-ray, neutron, and electron diffraction. The main results are presented here, and particular emphasis is put on those structural features in connection with the oxide−ion conductivity property.

Experimental Section

Synthesis. The oxide $La_2Mo_2O_9$ was prepared from a mixture of La_2O_3 and MoO_3 in the stoichiometric composition 1:2. The weighted powder was mixed in an agate mortar and then placed in an alumina crucible. This crucible was first heated at 500 °C for 12 h, then kept at 850−900 °C for several hours, and finally cooled slowly. Several regrindings and heatings were necessary to obtain a pure compound. The final product is white at room temperature and yellow at high temperature.

Structural Characterization. The X-ray and neutron powder diffraction patterns were recorded at different temperatures between 25 and 700 °C on a Bragg−Brentano X-ray diffractometer (Bruker-AXS D8) and Debye−Scherrer neutron diffractometer D1B (CRG-CNRS instrument operating at the ILL); details of data collection are presented in Table 1. A series of neutron diffraction patterns were collected between room temperature and 620 °C (wavelength 2.52 Å). Three long

* To whom correspondence should be addressed.
† Address: Laboratoire de Cristallographie, BP 166, 38042 Grenoble Cedex 9, France.

(1) Steele, B. C. H.; Oxygen ion conductors. In *High Conductivity Solid Ionic Conductors, Recent Trends and Applications*; Takahashi T., Ed.; World Scientific Publishing Co. Pte. Ltd.: Singapore, 1989; pp 402−446.
(2) Boivin, J. C.; Mairesse, G. *Chem. Mater.* **1998**, *10*, 2870−2888.
(3) Kendall, K. R.; Navas, C.; Thomas, J. K.; zur Loye, H.-C. *Solid State Ionics* **1995**, *82*, 215−223.
(4) Lacorre, Ph.; Goutenoire, F.; Bohnke, O.; Retoux, R.; Laligant, Y. *Nature*, **2000**, *404*, 856−858.
(5) Fournier, J. P.; Fournier, J.; Kohlmuller, R. *Bull. Soc. Chim. Fr.* **1970**, 4277.
(6) Lacorre, P.; Retoux, R. *J. Solid State Chem.* **1997**, *132*, 443−446.
(7) Goutenoire, F.; Retoux, R.; Suard, E.; Lacorre, P. *J. Solid State Chem.* **1999**, *142*, 228−235.
(8) Kuang, W.; Fan, Y.; Yao, K.; Chen, Y. *J. Solid State Chem.* **1998**, *140*, 354−360.

10.1021/cm991199l CCC: $19.00
Published on Web 08/15/2000

Table 1. Conditions of X-ray and Neutron Data Collection for $La_2Mo_2O_9$ Structural Determination

diffractometer	Bruker-AXS D8	D1B (ILL)
radiation	X-ray Cu Kα	neutron 1.28−2.52 Å
2θ range	15-120°	12.5°-91.85°
step-scan increment	0.02°	0.2°
counting time	40 s/step	total 12 h for long run; total 5 mn for short run

run diagrams were collected at low (room temperature), medium (533 °C), and high (617 °C) temperature (wavelength 1.28 Å). In all cases, the sample was put in a silica glass container under air. For the structural determination, atomic positions were located through Patterson function analysis and Fourier syntheses, using alternatively the programs FullProf,[9] ShelxS86, and ShelxL93.[10]

The electron diffraction study on the low-temperature form was performed on a 200 kV side entry JEOL 2010 electron microscope with a double tilt specimen holder operating at room temperature.

Crystal Structure of the High-Temperature Form (β-$La_2Mo_2O_9$). Given the complexity of the diffraction patterns of the room temperature α form of $La_2Mo_2O_9$ (see below), we have decided to focus first on the cubic form β.

Structural Determination. Both X-ray and neutron diffraction patterns of β-$La_2Mo_2O_9$ could be indexed on the basis of a cubic cell with a parameter $a = 7.2014(7)$ Å at 617 °C. The only extinction observed is for the $h00$ diffraction peaks, leading to the $h00$ $h = 2n$ existence condition, which suggests $P2_13$ (no. 198) and $P4_232$ (no. 208) as possible space groups.

The ab initio structural determination was carried out in the cubic system. To locate heavy atoms first, the integrated intensities were extracted, by the full pattern decomposition method of program Fullprof, from the X-ray diffraction pattern. The Patterson function was calculated using ShelxS86 program.[10] By taking account of the cell volume, the typical density of such oxides and the supposed oxygen stoichiometry of our compound, we assumed that $Z = 2$, which leads to a formula $La_4Mo_4O_{18}$ per unit cell, involving a calculated density $d_{calc} \approx 5.53$. In this hypothesis the simplest attempt was to start the structure determination with a 4-fold atomic position.

In the $P4_232$ space group the only positions with multiplicity 4 are 4b ($^1/_4$, $^1/_4$, $^1/_4$), and 4c ($^3/_4$, $^3/_4$, $^3/_4$). A structural model based on space group $P4_232$ with a molybdenum in 4b and a lanthanum in 4c did not lead to a good fit of the diffraction data. In space group $P2_13$, the only atomic position with multiplicity 4 is 4a (x,x,x). The Patterson function analysis gave a strong peak in (X,X,X) leading to two possible positions (x,x,x) and ($-x,-x,-x$). A good similarity between the observed and calculated patterns is obtained with a structural model based on such cationic positions, with $x = 0.14$. Two oxygen positions were then found by Fourier synthesis. These positions are 4a (oxygen O1) and 12b (oxygen O2). At this stage, we used the long-run neutron diffraction pattern. We started from the structural solution based on X-ray data; the atomic positions and anisotropic thermal factors were refined. The reliability factor was lowered to $R_{Bragg} = 11.4\%$ (see Table 2, model A). The refined composition corresponds to $La_4Mo_4O_{16}$, with two oxygen atoms missing relative to the compound's formulation $La_4Mo_4O_{18}$.

Attempts to locate the two extra oxygen atoms, which should be located on a site with partial occupation since 12a and 4b are the only available sites for space group $P2_13$, were only partly successful. Some extra atomic density on a 12b position could be found by Fourier difference analysis (oxygen O3). When occupancy is refined, being constrained with that of oxygen O2 site to fulfill oxygen stoichiometry, reliability is significantly lowered to $R_{Bragg} = 5.2\%$ (see Table 2, model B). However, a short O2−O3 distance precludes such a possibility, since the total occupancy of both sites (14) is larger than 50% of the maximal occupancy (24). When such a total occupancy is constrained to 50% of the maximal occupancy (stoichiometry $La_4Mo_4O_{16}$), thus lifting the distance condition, reliability slightly increases to $R_{Bragg} = 5.5\%$ (see Table 2, model C), which appears to be much lower than that of model A.

Further attempts to locate the extra two oxygen atoms were unsuccessful. Another possibility was tested, that of a deficiency on the cationic sublattice. Fixing it to 3.556/4 ($La_{3.556}Mo_{3.556}O_{16} = La_4Mo_4O_{18}$) leads, after refinement, to a reliability $R_{Bragg} = 5.8\%$ (see Table 2, model D, Table 3, and Table 4 for a list of La−O and Mo−O distances; see also Figure 1 for the fit). However, the small difference between the reliabilities of models B, C, and D incites us to be careful in the interpretation of these results, especially if we consider that the number of refined parameters is very high when compared to the number of observed reflections. The nature of the compound (oxide−ion conductor) and of the data (powder diffraction) does not allow one to be firmly conclusive about the exact atomic location.

Crystal Structure and Oxygen Conduction. Such a difficulty as locating conducting ions is rather common in ionic conductors due to the strong delocalization of such atoms. It can be evidenced by the strong decrease of the diffracted intensities

Table 2. Crystallographic Parameters of β-$La_2Mo_2O_9$ (T = 617 °C; Space Group: $P2_13$ (No. 198), $Z = 2$, Cell Parameters $a = 7.2014(5)$ Å)

atom (site)		model A: $La_2Mo_2O_8$	model B: $La_2Mo_2O_9$	model C: $La_2Mo_2O_8$	model D: $La_2Mo_2O_9$
La (4a)	x	0.8505(7)	0.8509(5)	0.8488(7)	0.8488(8)
	Occ	1	1	1	0.889
	B_{eq} (Å^2)[a]	3.8(3)	4.9(4)	5.1(4)	4.8(4)
Mo (4a)	x	0.179(1)	0.166(2)	0.167(2)	0.167(1)
	Occ	1	1	1	0.889
	B_{eq} (Å^2)[a]	3.6(2)	4.5(2)	5.5(3)	4.6(3)
O1 (4a)	x	0.331(3)	0.312(2)	0.312(2)	0.314(2)
	Occ	1	1	1	1
	B_{eq} (Å^2)[a]	14.9(9)	7.8(4)[b]	10.0(5)	11.8(6)
O2 (12b)	x	0.986(1)	0.987(1)	0.980(2)	0.983(2)
	y	0.153(2)	0.179(3)	0.163(7)	0.168(5)
	z	0.330(2)	0.332(3)	0.327(4)	0.330(3)
	Occ	1	0.82(2)	0.75(2)	0.73(2)
	B_{eq} (Å^2)[a]	9.7(9)	8.7(8)	13(2)	11(2)
O3 (12b)	x		0.923(4)	0.919(5)	0.911(6)
	y		0.621(6)	0.608(4)	0.612(5)
	z		0.558(4)	0.556(4)	0.554(4)
	Occ		0.34(2)	0.25(2)	0.27(2)
	B_{eq} (Å^2)[a]		11(1)[b]	7(3)	9(3)
R_{Bragg} (%)		11.4	5.2	5.5	5.8

[a] $B_{iso} = {}^4/_3\ a^2\ (\beta_{11} + \beta_{22} + \beta_{33})$. [b] Isotropic B thermal factors

Table 3. Anisotropic Thermal Parameters (×10^3) and Reliability of the Structural Refinement of β-$La_2Mo_2O_9$ (Model D, 617 °C)[a]

atom	β_{11}	β_{22}	β_{33}	β_{12}	β_{13}	β_{23}
La	23(2)	β_{11}	β_{11}	0(2)	β_{12}	β_{12}
Mo	22(1)	β_{11}	β_{11}	−5(2)	β_{12}	β_{12}
O1	57(3)	β_{11}	β_{11}	−6(3)	β_{12}	β_{12}
O2	7(3)	119(11)	37(4)	−1(4)	9(3)	38(9)
O3	63(22)	30(12)	35(7)	25(12)	43(10)	5(7)

[a] Reliability factors: $R_{Bragg} = 5.8\%$, $R_p = 10.9\%$, $R_{wp} = 6.5\%$, $R_{exp} = 2.3\%$, $\chi^2 = 7.7$, no. of reflections = 119, no. of refined parameter = 35.

(9) Rodriguez-Carvajal, J.; *Fullprof*, Version 3.5d, 1998.

(10) Sheldrick, G. M.; ShelxS86. In *Crystallographic Coumputing 3*; Sheldrick, G. M., Krüger, C., Goddards, R., Eds.; Oxford University Press: Oxford, 1985. Sheldrick, G.; *ShelxL93: A Program for Refinement of Crystal from Diffraction Data*; University of Göttingen: Göttingen, 1993.

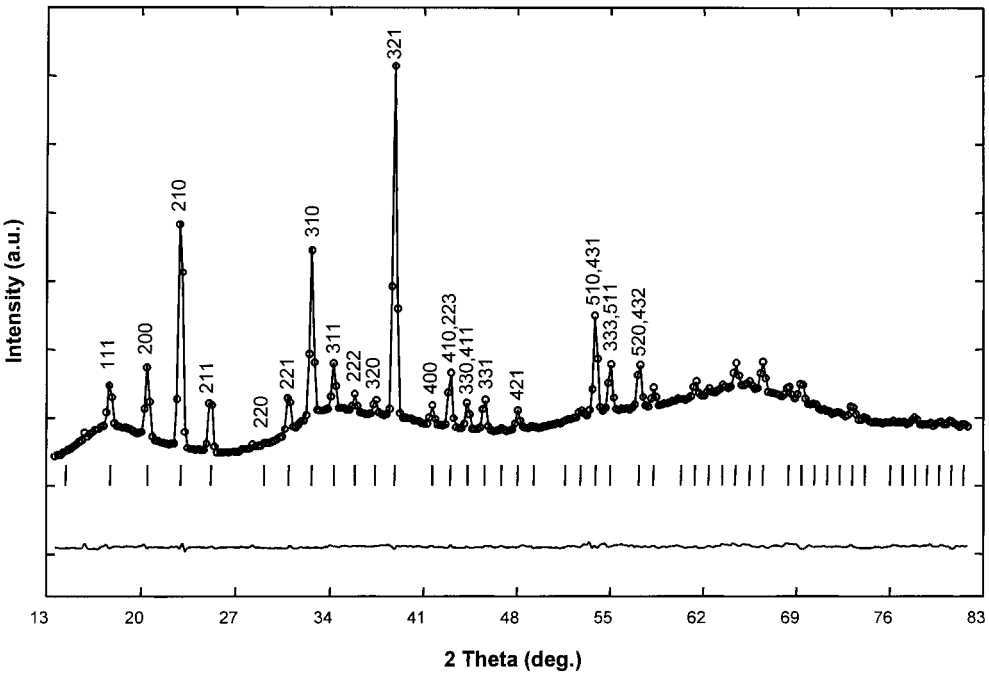

Figure 1. Fit corresponding to the final refinement of the structure of β-$La_2Mo_2O_9$ (from data collected at 617 °C, neutrons, D1B, $\lambda = 1.28$ Å), with observed (circles), calculated (line), and difference (lower) patterns. The strong modulated background is in this case due to the diffusion from the glass container.

Table 4. Selected Bond Distances (Å) for β-$La_2Mo_2O_9$ (Model D, $T = 617$ °C)

La Polyhedron	
La−O2	2.40(4) [×3][a]
La−O3	2.66(4) [×3][a]
La−O1	2.71(2) [×3]
La−O3	2.76(4) [×3][a]
La−O2	2.92(2) [×3][a]
Mo Polyhedron	
Mo−O3	1.73(4) [×3][a]
Mo−O2	1.77(3) [×3][a]
Mo−O1	1.83(2) [×1]

[a] O2 and O3 sites are partially occupied.

with the diffraction angle, leading to large thermal factors, especially for oxygen atoms. Such a decrease of the neutron diffraction intensities is straightforward (see Figure 1), and the corresponding large thermal factors of oxygen atoms are clearly evidenced in the current refinement (see Table 2). In our case, all oxygen atoms have large thermal factors, the conductivity being most probably three-dimensional in nature. The oxygen equivalent isotropic thermal factors for O1, O2, and O3 are respectively 11.8, 11.3, and 8.8 Å^2. These high thermal factors can be compared to those of other fast oxide−ion conductors. For example, the oxygen atoms around molybdenum atoms in $Bi_{23}Mo_{10}O_{69}$, a 1D oxide−ion conductor, exhibit thermal factors between 5.3 and 11 Å^2 at room temperature.[11] By comparison, in the high-temperature form of La_2O_3 (H form $T = 2030$ °C), the oxygen atoms present thermal factors between 15.8 and 17.9 Å^2.[12]

Another signature of oxygen diffusion can be found in a modulated neutron diffraction background:[11,12] a structural oxygen disorder is likely to originate from oxygen diffusion, which leads to short-range order. The background intensity of neutron diffractograms includes a contribution of elastic diffuse scattering coming from local static structural disorder.[13] To detect it, we collected a neutron diffraction pattern at room temperature (α form) in a regular vanadium container. This

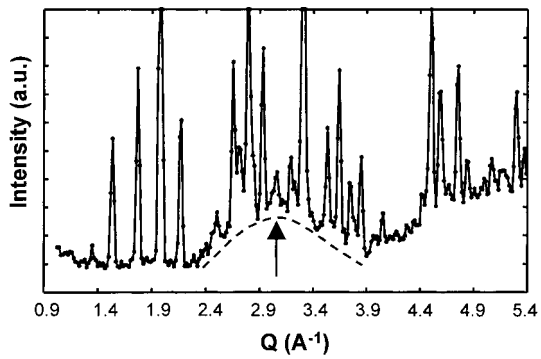

Figure 2. Detail of the neutron diffraction pattern of $La_2Mo_2O_9$ at room temperature versus $Q = 4\pi \sin\theta/\lambda$, showing a large diffusion peak around 2.31 Å^{-1} (due to short range order with pair distances around 2.5 Å). Note that the container contribution to the background is negligible (vanadium container).

pattern (free from any diffuse scattering of the container) allowed a careful examination of the diffraction background due to the sample, which exhibits a strong modulation with a first maximum around $Q = 3.1$ Å^{-1} (see Figure 2). The Debye formula can be used to express the contribution of static structural disorder in diffuse elastic scattering.[11] It exhibits a first marked maximum for $Q_{max} = (2\pi \times 1.23)/d_m$, where d_m is a preferred pair distance. When applied to our data, such a formula gives a preferred pair distance around 2.5 Å, which is characteristic of shortest oxygen−oxygen distances. This can be considered as a good confirmation of some oxygen short-range order in this compound.[11]

Structural Analysis. In β-$La_2Mo_2O_9$, La and Mo cations alternate to form a lattice of slightly distorted parallelepipeds, and define buckled (LaMo) planes perpendicular to the three main crystallographic axes (see Figure 3a). As already mentioned in ref 4, such an arrangement is reminiscent of that observed in the monazite structural type ($LnPO_4$), since it can

(11) Vannier, R. N.; Abraham, F.; Nowogrocki, G.; Mairesse, G. *J. Solid State Chem.* **1999**, *142*, 294−304.
(12) Aldebert, P.; Dianoux, A. J.; Traverse, J. P. *J. Phys.* **1979**, *40*, 1005−1012.
(13) Fender, B. E. F. In *Chemical Applications of Thermal Neutron Scattering*; Willis, B. T. M.; Ed.; Oxford University Press: London, 1974; pp 250−270.

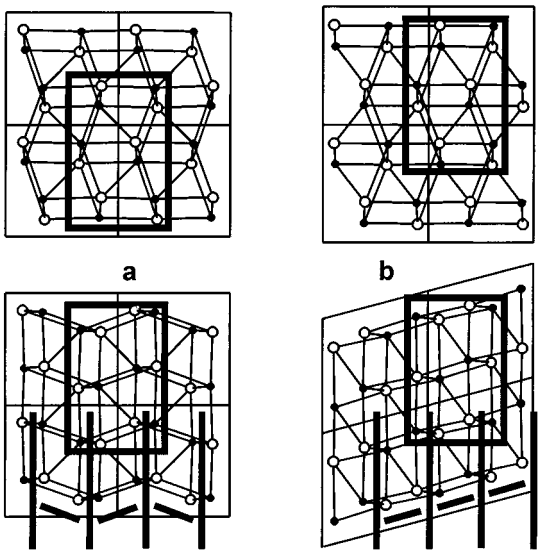

Figure 3. Cationic arrangement in the crystal structure of β-$La_2Mo_2O_9$ (a) compared to that of the monazite-type crystal structure of $LnPO_4$ (b) along two different crystallographic directions. Lanthanide atoms are represented by open circles, and countercations (Mo or P) by black circles. Common units of the two structures are surrounded. The microtwinning relationship is evidenced (see text).

be described as a microtwinning of the cationic arrangement of the monazite structure (see Figure 3b). A closer relationship exists with the crystal structure of the high-temperature cubic β form of $SnWO_4$ (ref 14), which crystallizes in the same space group $P2_13$ and adopts the same type of cationic arrangement. In this compound, however, the oxygen stoichiometry is different due to a lower cationic oxidation state. In β-$SnWO_4$, the lone pair of Sn^{2+} distorts its octahedral environment. It is usually considered that a lone pair occupies a volume similar to that of an O^{2-} anion.[15] This consideration allows us to propose an elementary model to explain the origin of oxide−ion conduction in $La_2Mo_2O_9$. Starting from tin 2+ tungstate and taking into account the Sn^{2+} lone pair (L), the stoichiometry can be reformulated $SnM^{6+}O_4L$, or $Sn_2M_2O_8L_2$. Substituting Sn^{2+} by La^{3+}, a cation of approximately the same size but without a lone pair, creates two extra vacancies, one of them being occupied by the extra oxygen which compensates for the cationic valence increase ($L_2 \rightarrow \square + O$). The new formula thus becomes $La_2M_2O_{8+1}\square$ and the extra vacancy allows for the oxide−ion conduction. Such a property is certainly favored by the ability of Mo^{6+} to adopt a distorted environment with various possible coordinations (4 to 6).

It is interesting to compare the cationic environments in β-$SnWO_4$ and β-$La_2Mo_2O_9$. In β-$SnWO_4$, the tungsten coordination polyhedron is a tetrahedron (see bottom of Figure 4a), with one oxygen atom on the 3-fold axis (site 4a, like W), and the three others away from it (site 12b). In β-$La_2Mo_2O_9$, the molybdenum coordination is modified as follows (see bottom of Figure 4b): while the 4a site remains fully occupied, the 12b site is partially occupied ($\sim^2/_3$) and Mo has moved toward the center of the corresponding triangular face. Extra oxygen O3, split on a 12b position ($\sim^1/_3$ occupied) is located on the other side of the triangular face relative to the fully occupied site 4a. Mo−O distances range between 1.73 and 1.83 Å. In β-$SnWO_4$, tin is in octahedral coordination, but the octahedron is very distorted (3 O at 2.21 Å and the 3 others at 2.81 Å, defining a larger triangular face), the lone pair pointing through the large triangular face (see top of Figure 4a). By comparison, in β-$La_2Mo_2O_9$ the corresponding octahedron around lanthanum is less distorted, and extra oxygen O3

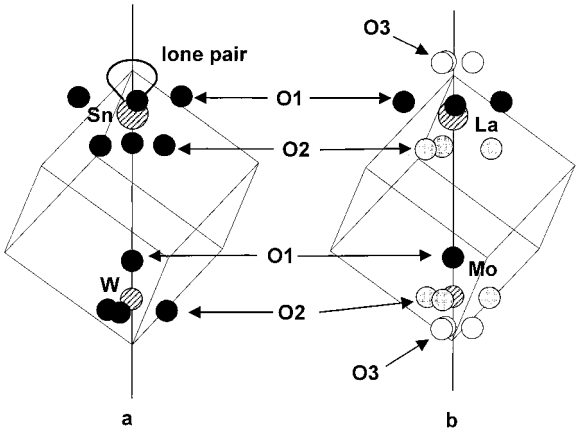

Figure 4. Cationic environments in β-$SnWO_4$ (a) and β-$La_2Mo_2O_9$ (b). For comparison purposes, the environment of La is limited to the nearest neighbors. Gray and open circle oxygen sites are partially occupied (see text).

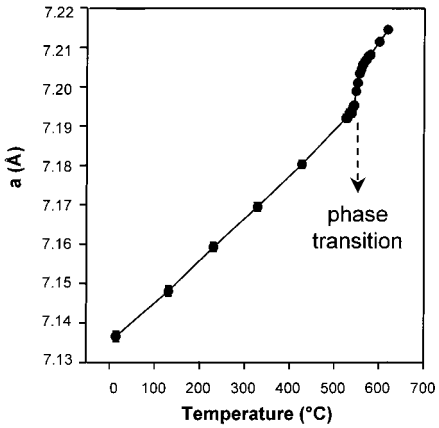

Figure 5. Thermal evolution of the (pseudo)cubic cell parameter of $La_2Mo_2O_9$, from low-resolution neutron diffraction data.

partially occupies the position of the lone pair in β-$SnWO_4$ (see top of Figure 4b). This last point confirms our model for the origin of oxide−ion conduction in $La_2Mo_2O_9$. La−O distances range between 2.40 and 2.92 Å.

In conclusion to this section, it can be said that the crystal structure of $La_2Mo_2O_9$ is different from that of any other known fast oxide−ion conductor. We thus deal here with a new family of oxide−ion conductors. Comparison with the structure of β-$SnWO_4$ provides a model for the origin of ionic conduction in the molybdate. More importantly, it suggests a recipe to design new oxide−ion conductors: the substitution, in ternary oxides, of lone-pair elements (oxidation state $+n$) by same size non-lone-pair ones with a higher oxidation state ($n + 1$). For each element, the lone pair is thus replaced by half a vacancy and half an oxygen atom, which is likely to migrate through the vacancy. The ability of the countercation to sustain a flexible coordination (as for instance Mo^{6+}) is probably a prime necessity.

Low-Temperature Form (α-$La_2Mo_2O_9$). In agreement with our previous study,[4] neutron thermodiffractometry confirmed the existence of a phase transition around 580 °C in $La_2Mo_2O_9$. The low resolution of the D1B instrument did not allow the detection of any diffraction peak splitting. Consequently, the low-T patterns could be indexed in a pseudocubic cell, whose thermal evolution of the parameter across the transition is plotted on Figure 5. A step in the cell parameter evolution is clearly visible at the phase transition, with an increase for the more conducting, high-temperature phase.

However, room-temperature high-resolution X-ray diffraction showed the existence of a splitting of most of the

(14) Jeitschko, W.; Sleight, A. W. *Acta Crystallogr.* **1972**, *B28*, 3174−3178.

(15) Wells, A. F.; *Structural Inorganic Chemistry*, 5th ed.; Oxford University Press; New York, 1987; p 1187.

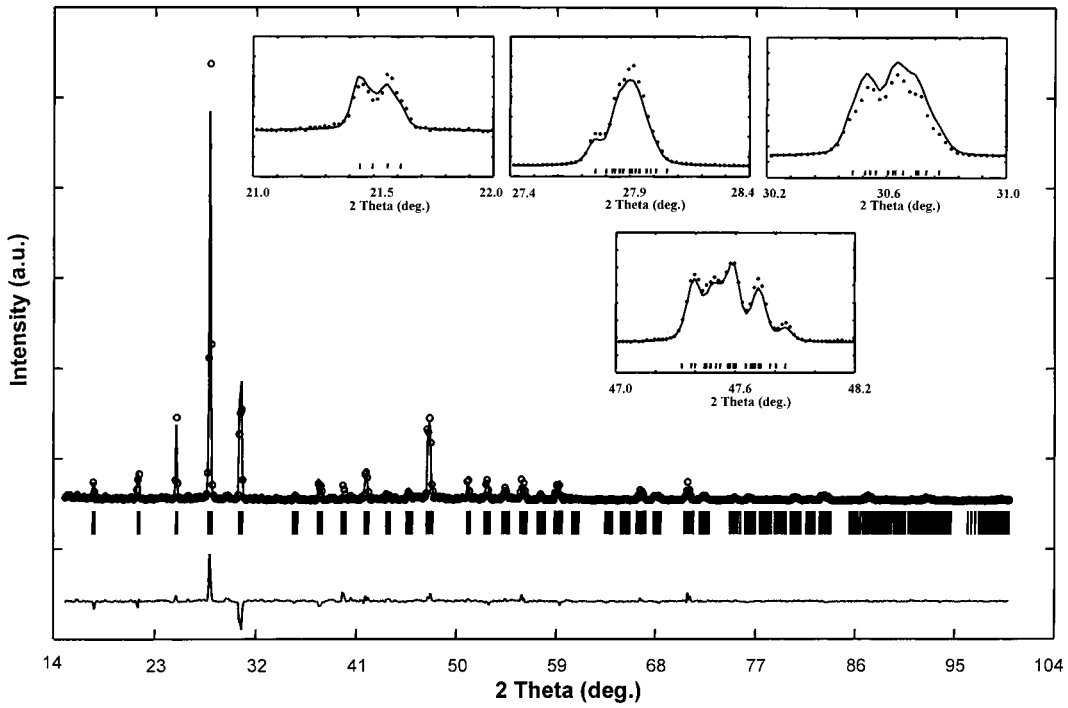

Figure 6. Fit corresponding to the refinement of the cationic arrangement of α-$La_2Mo_2O_9$ in a single monoclinic cell (from data collected at room temperature, high-resolution X-ray diffraction), with observed (circles), calculated (line), and difference (lower) patterns. Zoom of different ranges showing the splitting of diffraction peaks. These peaks correspond to the cubic (111), (210), (211), and (321) reflections.

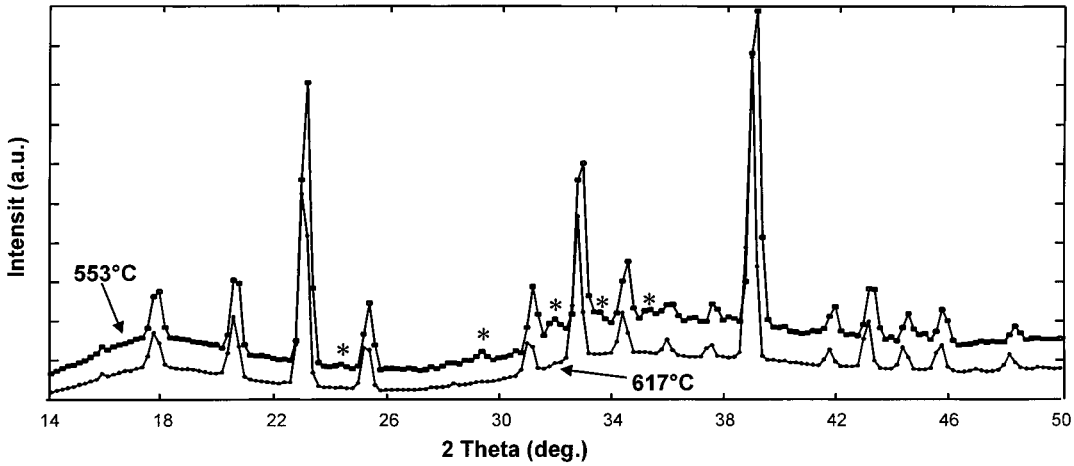

Figure 7. Neutron diffraction patterns of $La_2Mo_2O_9$ collected below (533 °C) and above (617 °C) the phase transition (D1B, λ = 1.28 Å). The stars point out the small extra peaks of α-$La_2Mo_2O_9$. These peaks probably correspond to the superstructure reflections observed in electron diffraction patterns.

diffraction peaks in α-$La_2Mo_2O_9$ (see insert Figure 6). Therefore, α-$La_2Mo_2O_9$ has a lower symmetry than the high-temperature, cubic form β-$La_2Mo_2O_9$. In addition, very small extra peaks were detected both in the X-ray and neutron diffraction patterns (see Figure 7), which is an indication of the existence of a superstructure relative to β-$La_2Mo_2O_9$.

As a first step, we neglected the superstructure peaks and attempted a pattern fitting, assuming a distortion of the small cubic cell. The X-ray diffraction pattern could not be accurately fitted in any orthorhombic distortion of the small cell, which would induce the presence of less diffraction peaks than effectively observed (this does not preclude the possibility of a larger orthorhombic cell). On the other hand, a good fit could be obtained in a monoclinic cell with parameters: a = 7.1426(5) Å, b = 7.1544(5) Å, c = 7.1618(5) Å and β = 89.538(3)°.

The room-temperature electron diffraction patterns of α-$La_2Mo_2O_9$ are presented on Figure 8; they show intense dots which can be indexed in a cubic cell with a parameter close to 7.15 Å. Nevertheless there is a large number of small dots which involve a superstructure. From reciprocal lattice reconstruction performed on several crystals, this superstructure can be described as $2a \times 3a \times 4a$, where a is the parameter of the cubic cell ($a \approx 7.15$ Å). The slight monoclinic distortion, suggested by the X-ray diffraction study (see above), could not be detected on electron diffraction patterns, probably because of its very small magnitude (less than 0.5°).

Various attempts to fit the diffraction pattern in an orthorhombic distortion of a $2 \times 3 \times 4$ supercell were unsuccessful; therefore we think that the true symmetry is monoclinic, with a $2 \times 3 \times 4$ superstructure. From neutron diffraction patterns in the low-temperature form, several small extra peaks can be evidenced (Figure 7), which could not be indexed in a cubic or pseudo-cubic cell. Since these extra peaks are larger than their X-ray counterparts, they most probably originate from a specific distribution of oxygen atoms in the structure. This is consistent with an order−disorder type transition between the two forms, as already observed in other fast oxide−ion conduc-

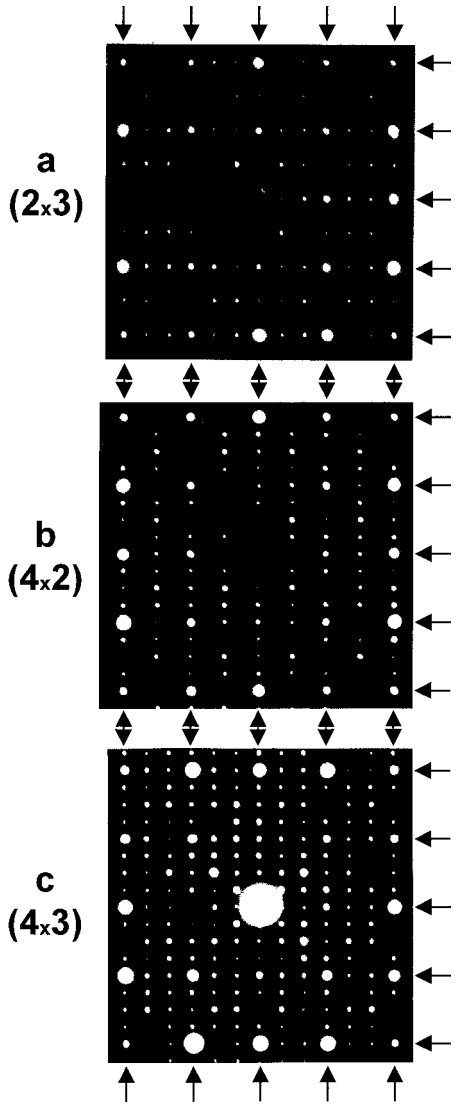

Figure 8. Electron diffraction patterns of α-$La_2Mo_2O_9$ along three perpendicular directions, showing the 2 × 3 × 4 superstructure relative to the cubic cell of β-$La_2Mo_2O_9$ (the main diffraction dots of the simple cubic lattice lie at the intersections of the horizontal and vertical arrows directions).

tors. Because of the poor resolution of the neutron diffraction pattern and because of the large cell volume $(7.15)^3 \times (2 \times 3 \times 4) \approx 8800$ Å^3, we did not try to determine the structure of α-$La_2Mo_2O_9$ in this large cell. We just attempted to locate cationic positions in the small monoclinic cell from the X-ray data. The symmetry was lowered from $P2_13$ to $P2_1$, and a (0.25,0.25,0) translation was applied to the atomic positions, to set the origin of the cell on the screw axis 2_1. The cationic model deduced from the structure of β-$La_2Mo_2O_9$ was refined, and reliability was lowered to $R_{Bragg} = 17.1\%$ (Figure 6). The complete determination of the crystal structure of α-$La_2Mo_2O_9$ is a challenge, and should be undertaken only after single crystals are available.

Summary and Conclusion

We have investigated the crystal structure of the high- and low-temperature forms of $La_2Mo_2O_9$, the parent compound of a new family of fast oxide−ion conductors, called LAMOX. The transition between the two forms takes place at 580 °C. The structure of the highly conducting high-temperature form has been determined ab initio using X-ray and neutron powder diffraction patterns. Two of the three located oxygen sites are partially occupied, and all of them exhibit large anisotropic thermal factors, in agreement with the observed oxygen diffusion, and strong static disorder of oxygen atoms as revealed by the undulated background of neutron diffractograms. The cationic positions can be considered as a microtwinning of those of the monazite structural type and correspond to those of β-$SnWO_4$. This last compound has allowed us to propose a structural model for the origin of oxide−ion conduction in $La_2Mo_2O_9$. More generally, it suggests that the substitution of a lone-pair cation by a non-lone-pair one with higher oxidation state could be used as a clue to design new fast oxide−ion conductors.

Because of oxygen localization, the less conducting α-$La_2Mo_2O_9$ exhibits a much more complex structure, with a monoclinic distortion and a 2 × 3 × 4 superstructure relative to β-$La_2Mo_2O_9$. Given the huge cell volume, such a challenging structure could not be determined from powder diffraction patterns.

More work is needed to fully characterize the structure and properties of the two forms of $La_2Mo_2O_9$, as well as those of the various other members of the new LAMOX family of fast oxide−ion conductors.

CM991199L